

# Efficacy and Selectivity of Phosphodiesterase-Targeted Drugs in Inhibiting Photoreceptor Phosphodiesterase (PDE6) in Retinal Photoreceptors

*Xiujun Zhang, Qing Feng, and Rick H. Cote*

**PURPOSE.** Phosphodiesterase (PDE) inhibitors are important therapeutic agents, but their effects on photoreceptor PDE (PDE6) and photoreceptor cells are poorly understood. The potency and selectivity of various classes of PDE inhibitors on purified rod and cone PDE6 and on intact rod outer segments (ROS) were characterized.

**METHODS.** The inhibition constant ( $K_i$ ) of isozyme-selective PDE inhibitors was determined for purified rod and cone PDE6. Perturbations of cGMP levels in isolated ROS suspensions by PDE inhibitors were quantitated by a cGMP enzyme-linked immunoassay.

**RESULTS.** Most PDE5-selective inhibitors were excellent PDE6 inhibitors. Vardenafil, a potent PDE5 inhibitor ( $K_i = 0.2$  nM), was the most potent PDE6 inhibitor tested ( $K_i = 0.7$  nM). Zaprinast was the only drug that inhibited PDE6 more potently than did PDE5. PDE1-selective inhibitors were equally effective in inhibiting PDE6. In intact ROS, PDE inhibitors elevated cGMP levels, but none fully inhibited PDE6. Their potency for elevating cGMP levels in ROS was much lower than their ability to inhibit the purified enzyme. Competition between PDE5/6-selective drugs and the inhibitory  $\gamma$ -subunit for the active site of PDE6 is proposed to reduce the effectiveness of drugs at the enzyme-active site.

**CONCLUSIONS.** Several classes of PDE inhibitors inhibit PDE6 equally as well as the PDE family to which they are targeted. In intact ROS, high PDE6 concentrations, binding of the  $\gamma$ -subunit to the active site, and calcium feedback mechanisms attenuate the effectiveness of PDE inhibitors to inhibit PDE6 and disrupt the cGMP signaling pathway during visual transduction. (*Invest Ophthalmol Vis Sci.* 2005;46:3060–3066) DOI:10.1167/iov.05-0257

Visual transduction is mediated by complex biochemical pathways that precisely regulate cGMP levels in the signal-transducing outer segment portion of vertebrate retinal photoreceptors (for reviews, see Refs. 1–3). Disruptions of cGMP metabolism in retinal photoreceptors have serious consequences for visual functioning. Most genetic mutations that are correlated with retinitis pigmentosa and related diseases are found in genes coding for proteins of the phototransduction

cascade, including photoreceptor phosphodiesterase (PDE6), guanylate cyclase (GC), and their associated regulatory subunits.<sup>4,5</sup> In many such cases, persistent elevation of cGMP concentration in retinal photoreceptors results in disruption of retinal development and/or photoreceptor apoptosis.

The rod and cone photoreceptor PDE6 belongs to a superfamily of 11 distinct cyclic nucleotide PDEs.<sup>6</sup> Rod and cone PDE6 is most closely related to PDE5—a cGMP-specific, cGMP-binding PDE—in structural, biochemical, and pharmacologic properties.<sup>7</sup> Drugs that selectively and potently target PDE5, such as sildenafil (Viagra; Pfizer, New York, NY), vardenafil (Levitra; Bayer Pharmaceuticals, New York, NY), and tadalafil (Cialis; Eli Lilly/ICOS [Bothell, WA], Indianapolis, IN), have been approved recently for treatment of male erectile dysfunction. These drugs represent the first major successful application of PDE inhibitor therapy to an individual family of PDEs, supplanting the nonspecific methylxanthine PDE inhibitors (e.g., theophylline and caffeine) used in the past.<sup>8–11</sup>

Remarkably little is known of the effects of PDE5-selective and other family-specific drugs on PDE6 and on cGMP metabolism in photoreceptors. Preclinical and clinical data on the effects of sildenafil have revealed significant but transitory effects on visual function, presumably through inhibition of photoreceptor PDE6.<sup>12</sup> Tadalafil and vardenafil, two other approved drugs, show lesser effects on visual function.<sup>13</sup> No systematic research of purified rod and cone PDE6 inhibition by various classes of PDE-selective inhibitors has been published in the literature, and only isolated data exist on potential differences between inhibition of the rod and cone PDE6 isozymes.<sup>14,15</sup> Electrophysiological measurements of individual rod photoreceptors exposed to IBMX (3-isobutyl-1-methylxanthine)<sup>16,17</sup> or zaprinast<sup>18</sup> demonstrate direct effects of PDE6 inhibition on the light responsiveness of rod photoreceptors, consistent with a drug-induced elevation in cGMP content.<sup>19</sup> Effects of PDE inhibitors on the electroretinogram or on human psychophysical measurements of visual function (reviewed in Ref. 12) are also consistent with direct inhibition of PDE6 in rods and cones.

In this study, we surveyed the potency and selectivity of PDE inhibitors targeted to PDE1 through -5, to inhibit purified rod and cone PDE6. We also examined the effects of nonselective and PDE5/6-selective inhibitors on cGMP concentration in the signal-transducing outer segment of rod photoreceptors. We found a general lack of discrimination of rod and cone photoreceptor PDE6 with respect to most drugs that have been designed to target a specific PDE family. However, in terms of the effectiveness of PDE inhibitors to elevate cGMP levels in intact ROS, we identified several mechanisms that oppose and minimize the ability of PDE inhibitors to disrupt cGMP metabolism in photoreceptor cells.

## METHODS

### Materials

Frogs (*Rana catesbeiana*) were obtained from Charles Sullivan, Inc., and kept in controlled lighting conditions (12 hours dark–light) for 2

From the Department of Biochemistry and Molecular Biology, University of New Hampshire, Durham, New Hampshire.

Supported by National Eye Institute Grant EY05798, Bayer Healthcare AG, and the New Hampshire Agricultural Experiment Station, Scientific Contribution 2259.

Submitted for publication February 24, 2005; revised March 31, 2005; accepted April 6, 2005.

Disclosure: **X. Zhang**, Bayer Healthcare AG (F); **Q. Feng**, Bayer Healthcare AG (F); **R.H. Cote**, Bayer Healthcare AG (F)

The publication costs of this article were defrayed in part by page charge payment. This article must therefore be marked “advertisement” in accordance with 18 U.S.C. §1734 solely to indicate this fact.

Corresponding author: Rick H. Cote, Department of Biochemistry and Molecular Biology, University of New Hampshire, Durham, NH 03824; rick.cote@unh.edu.

weeks before use. Animals were treated in accordance with ARVO guidelines, and protocols were approved by the institutional animal care and use committee. Bovine retinas were purchased from W. L. Lawson, Inc. (Lincoln, NE); E4021 was a gift from Eisai Co., Ltd. (Tokyo, Japan); vardenafil was provided by Bayer Pharmaceuticals; and sildenafil and tadalafil were synthesized. All other reagents were from Sigma-Aldrich (St. Louis, MO). All PDE inhibitors were prepared as stock solutions in DMSO and diluted in buffer before use, so that the final concentration of DMSO was always <1%. Ringer's solution consisted of (in mM): 105 NaCl, 2 KCl, 2 MgCl<sub>2</sub>, 1 CaCl<sub>2</sub>, 5 glucose, and 10 HEPES (pH 7.5). The ROS homogenization buffer contained (in mM): 100 Tris (pH 7.5), 10 MgCl<sub>2</sub>, 0.5 EDTA, 1 dithiothreitol, 0.5 mg/mL BSA, and mammalian protease inhibitor cocktail (Sigma-Aldrich). PDE assay buffer contained 20 mM Tris (pH 7.5), 10 mM MgCl<sub>2</sub>, and 0.5 mg/mL BSA.

### PDE6 Purification and PDE Activity Assay

Membrane-associated bovine rod and soluble cone PDE6 was purified from frozen bovine retinas exactly as described recently.<sup>20</sup> Activation of rod and cone PDE6 was performed by limited trypsin proteolysis of the inhibitory  $\gamma$ -subunit.<sup>20</sup> Rod or cone PDE6 was incubated with each drug for 15 minutes at room temperature before addition of the substrate. PDE activity was measured by either a phosphate release microplate assay (2 mM cGMP, 0.2 nM PDE6) or by a radiotracer assay (1.0  $\mu$ M cGMP, 2.0 pM PDE6);<sup>21</sup> similar  $K_i$  values were obtained with both assays.

### Purification of Intact ROS and Preparation of ROS Homogenates

Intact frog ROS were purified on a discontinuous density gradient (Percoll; Amersham Pharmacia Biotech, Piscataway, NJ), as described previously.<sup>21,22</sup> In brief, ROS were detached from dark-adapted retinas by gentle shaking in Ringer's supplemented with 5% Percoll. The ROS were then purified by centrifugation in a discontinuous gradient consisting of 5%, 30%, 44%, and 60% Percoll. Intact ROS were recovered from the 44%/60% Percoll interface, and were judged to be >90% osmotically sealed as determined by exclusion of the dye didansylcysteine.<sup>23</sup> The total cGMP levels in these ROS (0.008  $\pm$  0.001 mole cGMP per mole rhodopsin;  $n = 16$ ) are similar to previous measurements of isolated photoreceptors<sup>22</sup> and photoreceptors attached to the retina.<sup>24</sup>

The concentration of rhodopsin in ROS suspensions was determined spectrophotometrically.<sup>25</sup> To buffer the intracellular free calcium concentration of ROS at their dark-adapted level (~500 nM for amphibian ROS<sup>26</sup>), intact ROS were incubated in Ringer's supplemented with 1.09 mM EGTA for 10 minutes before addition of a PDE inhibitor.

Homogenized ROS were prepared by pooling intact ROS with disrupted ROS (found at the 30%/44% Percoll gradient interface). The discontinuous density gradient was removed by dilution with Ringer's and subsequent centrifugation (1 minute at 3000g). The ROS pellet was resuspended in homogenization buffer and homogenized until no organelle structures were visible by phase-contrast microscopy.<sup>27</sup> ROS nucleotides (particularly cGMP) were depleted (>95% loss) by incubating homogenized ROS at 22°C for 1 hour.<sup>28</sup>

### cGMP Concentration Measurement

cGMP was extracted by quenching with 50% HCl/ethanol, followed by centrifugation. The acidic supernatant containing cGMP was dried in a vacuum concentrator. The cGMP concentration was determined by cGMP enzyme-linked immunoassay (Amersham Pharmacia Biotech) with reference to standards treated identically to the experimental samples.

### Data Analysis

$K_i$  was calculated from the sigmoidal concentration dependence curve, with the following equation<sup>29</sup>:  $K_i = IC_{50}/(1 + [S]/K_m)$ , where  $IC_{50}$  is the

concentration of inhibitor that reduces catalytic activity in vitro by 50%,  $S$  is the substrate concentration, and  $K_m$  is the Michaelis constant. The following  $K_m$ s were used: 14  $\mu$ M for purified bovine rod PDE6,<sup>30</sup> 7  $\mu$ M for purified bovine cone PDE6 (Valeriani BA, Cote RH, unpublished data, 2004), and 20 and 60  $\mu$ M for activated or nonactivated frog PDE6, respectively.<sup>31</sup> All experiments were repeated at least three times, and average results are reported as the mean  $\pm$  SD. Curve fitting was performed with the computer program SigmaPlot (SPSS, Inc., Chicago, IL).

## RESULTS

### Ability of PDE Inhibitors to Discriminate Photoreceptor PDE6 In Vitro

We first tested a set of nonspecific and family-specific PDE inhibitors for their ability to inhibit purified PDE6. Both rod and cone PDE6 was tested in the activated state, in which the inhibitory  $\gamma$ -subunit is absent. Dose-response curves were generated for each inhibitor, and the drug inhibition constant ( $K_i$ ) was calculated based on the  $IC_{50}$  and knowledge of the  $K_m$  for each enzyme.

Table 1 summarizes the results of testing 15 PDE inhibitors that represent both nonspecific inhibitors (e.g., IBMX) and class-specific inhibitors of PDE1 through PDE5. (Family-specific inhibitors of PDE7 through PDE11 are not currently available.) We found that inhibitors of PDE3 and PDE4 were much less potent in inhibiting rod or cone PDE6 than their own PDE families. The selectivity (defined as the ratio of inhibition constants for PDE6 versus PDE-X) ranged from 40 to 50 (for the PDE4 inhibitor rolipram) to ~300 (for the PDE3 inhibitor cilostamide) and up to 5700 for the PDE4 inhibitor YM976. The PDE2 inhibitor EHNA showed low potency and a modest ability to discriminate PDE2 from PDE6. In contrast, both PDE1 inhibitors tested (8-methoxymethyl-IBMX and vinpocetine) did not discriminate PDE1 from rod PDE6. 8-Methoxymethyl-IBMX showed a 10-fold selectivity for cone PDE6 compared with PDE1, although in neither case was the drug very potent (cone PDE6  $K_i = 0.4 \mu$ M). We conclude that vinpocetine and 8-methoxymethyl-IBMX are more accurately defined as PDE1/6-specific inhibitors.

Most of the so-called PDE5-selective inhibitors tested in this study should be considered PDE5/6 inhibitors (Table 1). Whereas vardenafil ( $K_i < 1$  nM) is the most potent inhibitor of PDE6, it showed only threefold selectivity or less for PDE5 over PDE6. Both E4021 and sildenafil are potent PDE6 inhibitors ( $K_i \leq 10$  nM), but also lack discrimination of PDE5 versus PDE6. Only tadalafil (selectivity ratio of 210 [cone PDE6] or 640 [rod PDE6]) and T-1032 (selectivity ratio, 20–60) represent authentic PDE5-selective inhibitors. Zaprinast, a first generation PDE5-targeted inhibitor (which also weakly inhibits PDE1 with a 10-fold higher  $K_i$ ), has 10-fold higher potency for PDE6 than for PDE5 (Table 1) and should be considered a "PDE6-selective" inhibitor.

When examining pharmacologic differences between rod and cone PDE6, we found that 8-methoxymethyl-IBMX and its parent compound, IBMX, showed a three to fourfold preference for inhibiting cone PDE6 compared to the rod isozyme. None of the inhibitors tested in Table 1 preferred binding to rod PDE6 compared with cone PDE6.

### Effect of PDE Inhibitors and Guanylate Cyclase Regulation on cGMP Levels in Intact ROS

We next assessed the effects of PDE inhibitors on cGMP levels in metabolically active, isolated rod photoreceptor suspensions. When 400  $\mu$ M IBMX was incubated with dark-adapted frog ROS in standard isolation conditions, a 20% elevation of

TABLE 1. The Efficacy and Selectivity of PDE Inhibitors to Inhibit Purified, Activated Bovine Rod and Cone PDE6

Class	Inhibitor	PDE(X) $K_i$ (nM)*	PDE6 $K_i$ (nM)†		Selectivity‡		
			Rod	Cone	6R/6C	6R/X	6C/X
1	Vinpocetine	11500	21000 ± 6100	13000 ± 1200	1.6	1.8	1.1
	8-Me-IBMX	3300	1600 ± 100	430 ± 30	3.7	0.5	0.1
2	EHNA	2500	28000 ± 2400	13000 ± 1600	2.2	11	5
3	Cilostamide	10	2800 ± 170	3400 ± 660	0.8	280	340
4	Rolipram	490	28000 ± 620	22000 ± 4000	1.3	57	45
	YM 976	3.3	19000 ± 1500	5200 ± 630	3.7	5760	1580
5	Tadalafil	3.3	2100 ± 150	700 ± 60	3.0	640	210
	Dipyridamole	580	480 ± 30	190 ± 14	2.5	0.8	0.3
	T-1032	1.2	75 ± 12	26 ± 7	2.9	63	22
	T-0156	23§	51 ± 4.0	61 ± 5	0.8	2.2	2.6
	Zaprinast	325	30 ± 3.0	32 ± 6	0.9	0.1	0.1
	Sildenafil	4.4	11 ± 1.0	4.7 ± 0.5	2.3	2.5	1.1
	E4021	2.9	2.9 ± 0.5	2.9 ± 0.5	1.0	1.0	1.0
	Vardenafil	0.25	0.71 ± 0.06	0.3 ± 0.03	2.4	2.8	1.2
	NS	IBMX	—	4490 ± 804	1410 ± 453	3.2	—

\* Average of  $K_i$  values for each family of PDE obtained from the literature. IBMX is nonselective (NS).

† The  $K_i$  was determined from the equation:  $K_i = IC_{50}(1 + [cGMP]/K_m)$ , where the  $IC_{50}$  was obtained from the dose-response curve for each inhibitor for rod and cone PDE6 and the  $K_m$  for bovine rod and cone PDE6 are 14  $\mu$ M or 7.0  $\mu$ M, respectively.

‡ Selectivity is defined as the ratio of the  $K_i$  for the two indicated PDEs: 6R, rod PDE6; 6C, cone PDE6, and; X, PDE families 1 through 5.

§ Reported value is the  $IC_{50}$ , because  $K_i$  could not be calculated.

cGMP levels was observed, compared with control ROS suspensions (Fig. 1). (A species difference in the potency of IBMX to inhibit PDE6 cannot account for this result, because the  $K_i$  of frog PDE6 [Table 2] is virtually identical with the  $K_i$  of bovine PDE6 [Table 1].)

Based on a similar report on the effects of IBMX on the cGMP content of rabbit retina where almost equal reductions in the rates of cGMP hydrolysis and synthesis were observed,<sup>32</sup> it seemed likely that inhibition of guanylate cyclase compensates for the inhibitory effects of IBMX on PDE6 in frog ROS in Figure 1. Because IBMX is known to elevate internal calcium concentrations in ROS<sup>33</sup> which would then inhibit the calcium-

sensitive guanylate cyclase, we decided to "clamp" the free calcium concentration of ROS at its dark-adapted level of ~500 nM. By itself, buffering the calcium concentration to 500 nM in the Ringer's solution elevated cGMP levels by ~50% (Fig. 1), consistent with an earlier study.<sup>34</sup> However, when preincubation with a calcium-buffered Ringer's was combined with treatment with 400  $\mu$ M IBMX, we observed a fivefold elevation of cGMP concentration in frog ROS (Fig. 1). Thus, IBMX inhibition of PDE6 in intact, dark-adapted ROS resulted in the elevation of cellular cGMP concentration when guanylate cyclase activity was held constant by buffering free calcium. To isolate the effect of PDE5/6 inhibitors on PDE6 in intact ROS, the remaining experiments were performed in buffered calcium conditions.

### Dose-Response Relationship of PDE Inhibitors on cGMP Levels in Intact ROS

To see whether high-potency PDE5/6 inhibitors behave differently from IBMX, we compared the time course of cGMP elevation when sildenafil, vardenafil, or IBMX were incubated with ROS maintained in a 500 nM calcium-Ringer's solution. Figure 2 shows that cGMP levels in ROS reached an elevated, stable plateau within 2 minutes after exposure to the PDE inhibitor. The relatively slow action of PDE inhibitors on cGMP metabolism in intact ROS contrasts with the instantaneous inhibition of purified, activated PDE6 by these drugs in vitro (data not shown), and the rapid (<1 second) inactivation of PDE6 inferred in electrophysiological recordings.<sup>35</sup> The new steady state level of cGMP after drug exposure suggests that PDE6 is not completely inhibited at the inhibitor concentrations tested in Figure 2.

We next determined the dose-response relationship of IBMX, sildenafil, and vardenafil on dark-adapted ROS maintained in a calcium-buffered Ringer's solution. For all three inhibitors, the aqueous solubility limit of each drug was reached before a plateau in the cGMP stimulation could be observed (Fig. 3). For 2.0 mM IBMX or 125  $\mu$ M vardenafil, a fivefold elevation of cGMP levels was observed (Fig. 3A), whereas 110  $\mu$ M sildenafil induced a less than twofold increase in cGMP content in ROS (Fig. 3B). Because no evidence of saturation was observed for these drugs, these concentrations

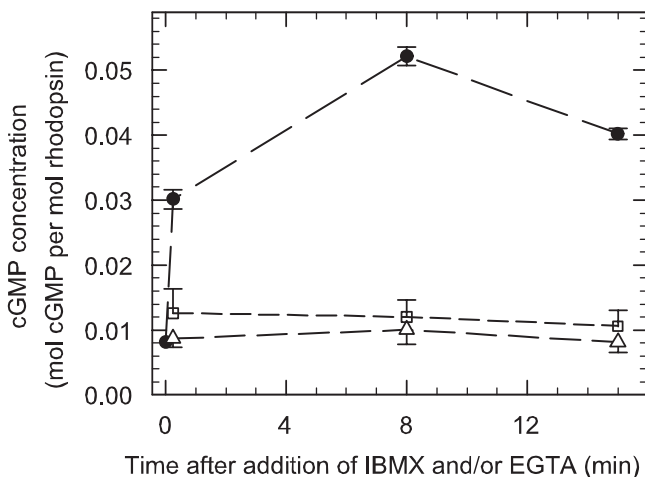


FIGURE 1. Synergistic effect of inhibiting PDE6 and buffering intracellular  $Ca^{2+}$  on cGMP levels in intact ROS. Purified ROS suspensions (rhodopsin, 4.8  $\mu$ M) were prepared in complete darkness. Two portions were incubated with either 1.09 mM EGTA ( $[Ca^{2+}]_{free}$ , 500 nM; squares) or 400  $\mu$ M IBMX (triangles). A third sample was first preincubated for 10 minutes with EGTA followed by addition of IBMX (circles). Portions were quenched at the indicated times with 50% HCl/ethanol. The cGMP concentration was determined by an enzyme-linked immunoadsorbent assay and reported relative to the rhodopsin content of the sample. Data points at the mean  $\pm$  SD of results in three experiments.

**TABLE 2.** Comparison of the Effects of IBMX and Vardenafil on Frog Rod PDE6 Catalytic Activity and on cGMP Levels of Intact Frog ROS

Inhibitor	Frog PDE6 $K_i$ ( $\mu\text{M}$ )*		Intact ROS ( $\mu\text{M}$ )†	
	Activated	Nonactivated	Observed $\text{EC}_{50}$	Predicted $\text{IC}_{50}$
IBMX	$4.3 \pm 0.5$	$14 \pm 1.3$	1000	73
Vardenafil	$0.0019 \pm 0.0004$	$0.022 \pm 0.004$	50	0.14

\* The  $K_i$  values were determined as described in Table 1, using nucleotide-depleted frog ROS homogenates to measure nonactivated (10  $\mu\text{M}$  cGMP, 4.0 nM PDE6) or activated (1.0  $\mu\text{M}$  cGMP, 20 pM PDE6) PDE6.

† Intact frog ROS (4.8  $\mu\text{M}$  rhodopsin) were prepared as described in the Methods section. The observed  $\text{EC}_{50}$  is an estimate from the results of Figure 3. The predicted  $\text{IC}_{50}$  was calculated with the equation:  $\text{IC}_{50} = K_i(1 + [\text{cGMP}]/K_m)$  where the nonactivated  $K_i$  is used, the cGMP concentration is the dark-adapted value for intact ROS (50  $\mu\text{M}$ ), and the  $K_m$  (60  $\mu\text{M}$ ) refers to the value for nonactivated frog PDE6 with cGMP as the substrate.<sup>31</sup>

represent a minimum estimate of the effective dose needed to produce a half-maximum change ( $\text{EC}_{50}$ ) in ROS cGMP levels.

The relative potency with which PDE inhibitors affected purified PDE6 catalysis in vitro (i.e.,  $K_i$ ) compared with the perturbing cGMP levels in intact ROS (i.e.,  $\text{EC}_{50}$ ) is difficult to quantify. However, for a first approximation, we can calculate the predicted  $\text{IC}_{50}$  for an inhibitor to block PDE6 activity in the presence of the cGMP concentration in dark-adapted ROS (50  $\mu\text{M}$ ), assuming no diffusional barriers. As shown in Table 2, the predicted  $\text{IC}_{50}$  for IBMX (73  $\mu\text{M}$ ) is at least 14-fold lower than the minimum  $\text{EC}_{50}$  estimated in Figure 3. In contrast, the predicted  $\text{IC}_{50}$  for vardenafil (140 nM) is at least 350-fold lower than the minimum  $\text{EC}_{50}$  for intact ROS.

### Competition between the Inhibitory $\gamma$ -Subunit and PDE Inhibitors at the Active Site of PDE6

In dark-adapted ROS, rod PDE6 exists in its nonactivated state in which the catalytic dimer ( $\alpha\beta$ ) is inhibited by binding of two inhibitory  $\gamma$ -subunits (for review, see Ref. 36). Figure 4 dem-

onstrates that vardenafil's inhibitory potency for the PDE6  $\alpha\beta\gamma_2$  holoenzyme is reduced 12-fold compared with the activated PDE6  $\alpha\beta$  catalytic dimer. In contrast, IBMX inhibition of PDE6 holoenzyme is reduced only threefold relative to activated PDE6. This discrepancy may be accounted for by competition between the  $\gamma$ -subunit and PDE inhibitor for a common binding site in the catalytic pocket (see the Discussion section).

To test this idea further, we examined the ability of IBMX, sildenafil, and vardenafil to compete at the active site, not only with cGMP but also with the  $\gamma$ -subunit. Figure 5 shows that at

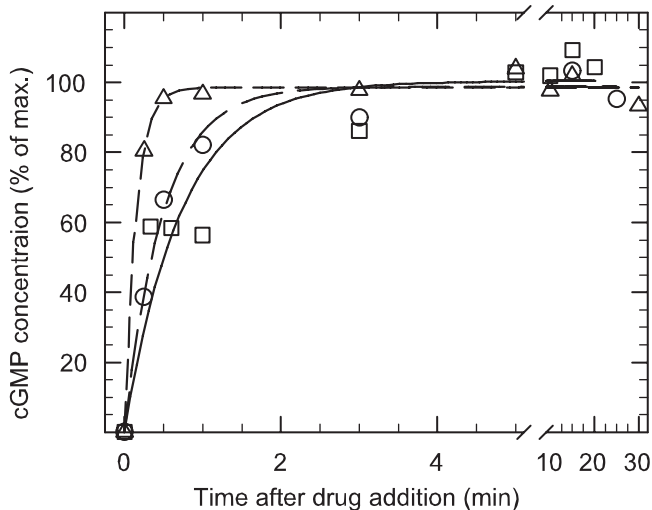


**FIGURE 2.** Time course of drug-induced increase in cGMP concentration in intact ROS. Purified ROS (0.008 mole cGMP per mole rhodopsin) were preincubated with 1.09 mM EGTA for 10 minutes, to buffer the free calcium concentration. At time 0, 400  $\mu\text{M}$  IBMX ( $\circ$ ), 50  $\mu\text{M}$  sildenafil ( $\Delta$ ), or 100  $\mu\text{M}$  vardenafil ( $\square$ ) was added and the samples quenched in 50% HCl/ethanol for cGMP determinations. The results were normalized to the average maximum stimulation for each drug (units: moles cGMP per mole rhodopsin): IBMX, 0.040; vardenafil, 0.035; and sildenafil, 0.014. Data points are the mean of results in three experiments in which the SD was  $\leq 13\%$  of the mean.

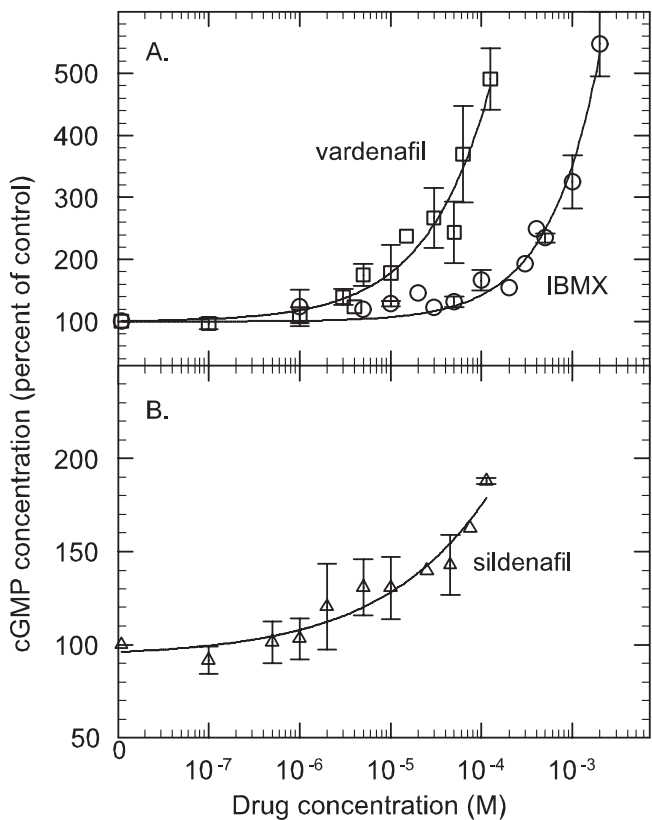


**FIGURE 3.** PDE inhibitors induced dose-dependent elevations of ROS cGMP levels that do not saturate.  $\text{Ca}^{2+}$ -buffered ROS suspensions (10-minute preincubation with 1.09 mM EGTA) were treated with the indicated concentration of IBMX ( $\circ$ ), sildenafil ( $\Delta$ ), or vardenafil ( $\square$ ) for 10 minutes and then acid quenched for cGMP extraction and quantitation. The data points are the mean  $\pm$  SD of results in three experiments.

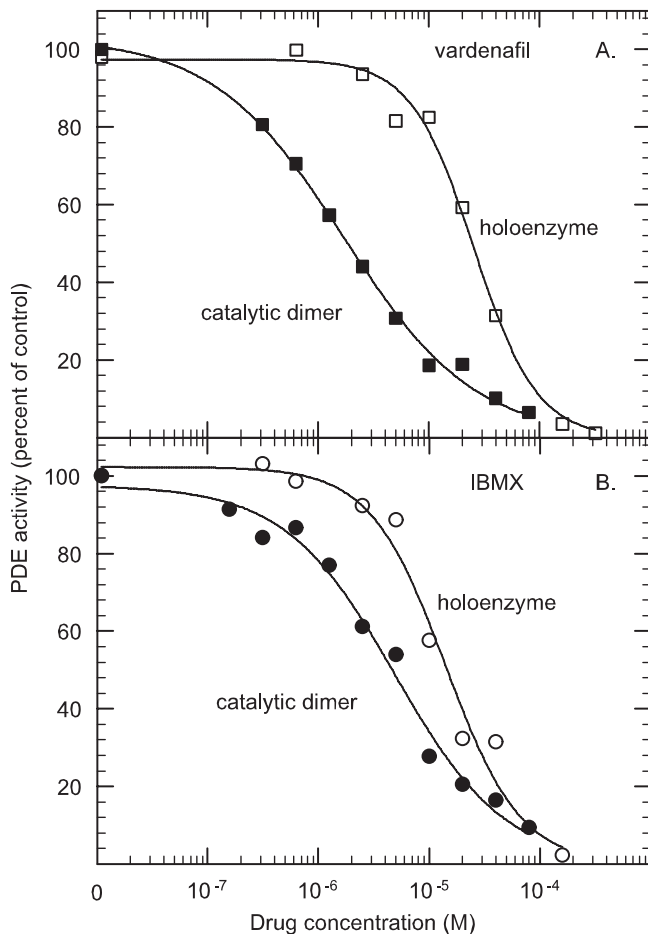


**FIGURE 4.** PDE6 holoenzyme was less susceptible to inhibition by PDE inhibitors. ROS suspensions were homogenized, and soluble proteins and metabolites were separated from PDE6-containing ROS membranes by centrifugation. The ROS membranes were further depleted of endogenous nucleoside triphosphates by incubation at 22°C for 30 minutes. Nonactivated PDE6 holoenzyme (4 nM; *open symbols*) was incubated with vardenafil (**A**) or IBMX (**B**) for 15 minutes before addition of 10  $\mu\text{M}$  [ $^3\text{H}$ ]cGMP, to assay catalytic activity. Activated PDE6 (20 pM; *filled symbols*) was incubated with vardenafil (**A**) or IBMX (**B**) for 15 minutes before adding 1  $\mu\text{M}$  [ $^3\text{H}$ ]cGMP. The results shown are typical of those in at least three other experiments.

low drug concentrations both vardenafil and sildenafil—but not IBMX—stimulated the PDE6 holoenzyme two- to threefold when 2 mM cGMP was used as the substrate. (This paradoxical stimulation of PDE6  $\alpha\beta\gamma_2$  activity at low drug concentrations was first observed with zaprinast<sup>14</sup> and E4021.<sup>37</sup>) At higher drug concentrations, the expected inhibitory action of all three inhibitors was seen. Under identical conditions, activated PDE6 catalytic dimers ( $\alpha\beta$ ) did not show stimulation of catalysis at low drug concentrations (data not shown). These results are consistent with high-affinity, bulkier PDE5/6 inhibitors competing with  $\gamma$ -subunit binding in the catalytic pocket, whereas the smaller IBMX molecule inhibits catalysis without greatly affecting  $\gamma$ -subunit binding (see the Discussion section).

## DISCUSSION

### Susceptibility of Photoreceptor PDE6 to Inhibition by PDE1-, PDE2-, and Most PDE5-Directed Drugs

A central issue in the clinical development of PDE inhibitor therapy is the specificity of the drug for the targeted PDE.

Table 1 is the first systematic analysis of the inhibition of rod and cone PDE6 by inhibitors that were designed to target PDE families 1 through 5. With the exception of PDE3- and PDE4-selective inhibitors and a few PDE5-selective inhibitors, most of the tested compounds in Table 1 lacked selectivity ( $K_i$  ratio  $< 10$ ) for the PDE family they are intended to target. The 10-fold selectivity of zaprinast for PDE6 compared to PDE5 makes this compound the only “PDE6-selective” inhibitor that we tested. The high selectivity of the PDE5 inhibitor tadalafil for PDE5 over PDE6 bodes well for future drug development in which vision-impairing side effects resulting from PDE6 inhibition may be minimized further.

None of the compounds we tested showed major differences in their inhibition of rod and cone PDE6 isozymes, although two xanthine analogues (IBMX and 8-methoxymethyl-IBMX) showed three- to fourfold selectivity for cone PDE6. Differences in amino acid residues contacting these inhibitors and/or differences in conformation of the active site<sup>38</sup> may explain this preference of cone PDE6 for xanthine-based inhibitors.

The ability of PDE6 to bind to several different classes of PDE inhibitor may reflect the unique catalytic properties of the photoreceptor enzyme. Unlike the other 10 PDE families, PDE6 operates with very high catalytic efficiency for cGMP ( $k_{\text{cat}}/K_m = 4 \times 10^8 \text{ M}^{-1} \cdot \text{s}^{-1}$ ; see Ref. 36). Although the low affinity of substrate ( $K_m = 20 \mu\text{M}$  for cGMP) and the high catalytic constant (up to 8000 cGMP hydrolyzed per second) of PDE6 are ideally suited for the millisecond time-scale activation of PDE6 required for visual transduction,<sup>2</sup> these same properties may allow a wide variety of inhibitor compounds to enter the catalytic pocket and inhibit catalysis.

### Modulation of the Effect of PDE Inhibitors on cGMP Levels in Photoreceptors

The observation that PDE inhibitors only modestly elevated cGMP levels in intact ROS unless the free calcium concentration was buffered (Fig. 1) can be explained as follows: Inhibition of PDE6 by drug entry into the outer segment transiently elevates cGMP levels. This causes cGMP-gated ion channels to

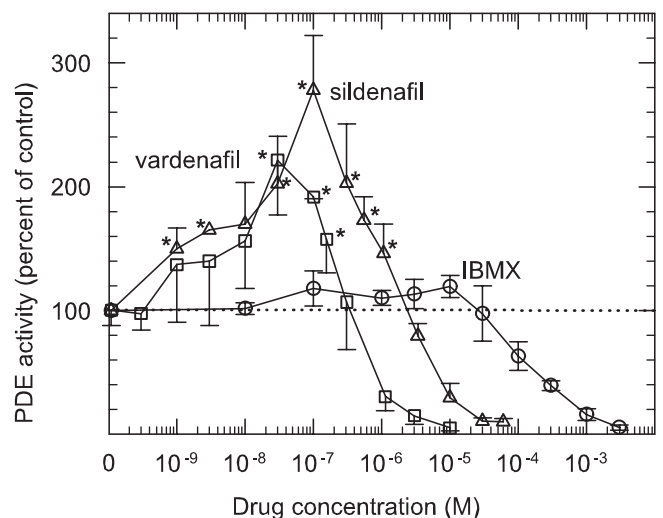


**FIGURE 5.** PDE5/6-selective inhibitors, but not IBMX, stimulated catalysis at high cGMP concentrations. ROS membranes (2.0 nM PDE6 concentration) depleted of soluble proteins and nucleotides were incubated with IBMX ( $\circ$ ), sildenafil ( $\Delta$ ), or vardenafil ( $\square$ ) for 15 minutes. Catalytic activity was determined by a colorimetric assay with 2 mM cGMP. The data were normalized to the basal PDE6 activity for plotting and represent the mean  $\pm$  SD ( $n = 3$ ). \*Statistically significant,  $P < 0.05$ .

open, allowing entry of sodium and calcium into the ROS. Elevation of intracellular calcium inhibits guanylate cyclase and offsets the reduced hydrolysis of cGMP by the inhibited PDE6, resulting in little or no increase in cGMP concentration.<sup>32</sup> On buffering free calcium in the medium, this calcium feedback mechanism is blocked, allowing continued synthesis of cGMP in conjunction with reduced cGMP hydrolysis, and a net increase in intracellular cGMP concentration.

The plateau in steady state cGMP levels after incubation of IBMX or PDE5/6-selective inhibitors with ROS suspensions (Fig. 2) was unexpected, because PDE6 inhibition in conjunction with continued cGMP synthesis by guanylate cyclase in the calcium-buffered Ringer's should lead to continual increases in intracellular cGMP concentration. Also unexpected was the failure of all tested PDE inhibitors to show saturation behavior when cGMP levels in ROS were assayed as a function of inhibitor concentration (Fig. 3). In contrast, both nonactivated and activated PDE6 in vitro displayed stereotypical dose-response behavior with IBMX or vardenafil (Fig. 4). Assaying PDE6 inhibition in situ in intact ROS (Fig. 3) must take into consideration the very high PDE6 concentration in the outer segment of rod photoreceptors (40  $\mu$ M catalytic subunit concentration in frog rods<sup>39</sup>). Although the high PDE6 concentration associated with the outer segment membranes facilitates the single-photon sensitivity of photoreceptors,<sup>40</sup> it also requires very high drug concentrations to stoichiometrically inhibit PDE6 in ROS. (For example, in Figure 3 the highest tested concentrations of sildenafil and vardenafil are only approximately threefold greater than the PDE6 subunit concentration in ROS.) In summary, the unexpected behavior illustrated in Figures 2 and 3 can be accounted for if some of the PDE6 in intact ROS cannot be inhibited under our experimental conditions.

### Role of the $\gamma$ -Subunit in Determining the Potency of PDE Inhibitors

In the case of the closely related PDE5 family of phosphodiesterases, allosteric activation of PDE5 by cGMP binding to the GAF domain enhances the binding affinity of sildenafil, tadalafil, and vardenafil.<sup>41,42</sup> Figure 4 demonstrates a parallel phenomenon for PDE6, wherein activated PDE6 catalytic dimer ( $\alpha\beta$ ) was more potently inhibited by PDE inhibitors than the nonactivated holoenzyme ( $\alpha\beta\gamma_2$ ). This effect was more pronounced for vardenafil (Fig. 4A) than for IBMX (Fig. 4B). Furthermore, low concentrations of sildenafil or vardenafil—but not IBMX—can cause an apparent stimulation of nonactivated PDE6 when the cGMP substrate concentrations are very high (Fig. 5). This latter effect is probably due to mutually exclusive competition between the  $\gamma$ -subunit, drug, and substrate for a common binding site in the catalytic pocket, in conjunction with an  $\sim$ 1000-fold greater affinity of  $\gamma$ -subunit ( $K_d \sim$  pM<sup>43,44</sup>) than of drug ( $K_i \sim$  nM; Tables 1, 2) for the active site.

These results have important implications for the architecture of the catalytic site of PDE6. IBMX, a xanthine derivative, has been shown to occupy a subpocket within the active site of PDE5 normally occupied by the guanine ring of cGMP<sup>38</sup> and exhibits many of the same interactions observed with the authentic substrate. Although IBMX, sildenafil, and vardenafil all share contact points in this region, the two PDE5/6-selective inhibitors also contact the catalytic pocket of PDE5 at additional sites that account for the 1000-fold higher affinity of these drugs.<sup>45</sup> Many of these PDE5 contacts interacting with the ethoxyphenyl and methoxypiperazine groups of sildenafil are close to amino acids that in PDE6 have been implicated in  $\gamma$ -subunit binding to the catalytic domain.<sup>46,47</sup> If the bulkier PDE5/6-selective inhibitors overlap in their binding sites with

the  $\gamma$ -subunit interaction sites in the catalytic pocket of PDE6, it would explain the mutually exclusive competition of  $\gamma$ -subunit and drug that weakened the affinity of these drugs for nonactivated PDE6 (Fig. 4) and led to the paradoxical activation of PDE6 holoenzyme at low drug concentrations (Fig. 5).

### CONCLUSIONS

In summary, when assessing the clinical efficacy of PDE inhibitor therapy for treatment of human diseases, the following effects on photoreceptor PDE6 must be considered: the ability of systemically administered PDE inhibitors to cross the blood-retinal barrier to reach the photoreceptors (not addressed in this study); the intrinsic pharmacologic selectivity of the drug for PDE6 inhibition; the unique cellular context of the rod outer segment in which PDE6 resides; the state of activation of PDE6 (and hence its competition with the  $\gamma$ -subunit); and the interrelatedness of cGMP and calcium metabolism in visual signaling. Regarding calcium, the fact that elevation of cGMP levels by PDE inhibitors increases intracellular calcium concentration in photoreceptors may have serious consequences, considering that photoreceptor apoptosis and retinal degeneration are believed to result from sustained cGMP elevation and/or calcium overload.<sup>48,49</sup> For these reasons, administration of PDE inhibitors for novel therapeutic uses must be evaluated for potential adverse effects on photoreceptor viability as well as visual function.

### Acknowledgments

The authors thank Bev Valeriani (University of New Hampshire) for providing the purified cone PDE6 used in some of the experiments.

### References

- Pugh EN, Lamb TD. Phototransduction in vertebrate rods and cones: molecular mechanisms of amplification, recovery and light adaptation. In: Stavenga DG, DeGrip WJ, Pugh EN, eds. *Molecular Mechanisms in Visual Transduction*. New York: Elsevier Science BV; 2000:183–255.
- Arshavsky VY, Lamb TD, Pugh EN Jr. G proteins and phototransduction. *Annu Rev Physiol*. 2002;64:153–187.
- Zhang X, Cote RH. cGMP signaling in vertebrate retinal photoreceptor cells. *Front Biosci*. 2005;10:1191–1204.
- Farber DB. From mice to men: the cyclic GMP phosphodiesterase gene in vision and disease. The Proctor Lecture. *Invest Ophthalmol Vis Sci*. 1995;36:263–275.
- Duda T, Koch KW. Retinal diseases linked with photoreceptor guanylate cyclase. *Mol Cell Biochem*. 2002;230:129–138.
- Francis SH, Turko IV, Corbin JD. Cyclic nucleotide phosphodiesterases: relating structure and function. *Prog Nucleic Acids Res Mol Biol*. 2001;65:1–52.
- Cote RH. Characteristics of photoreceptor PDE (PDE6): similarities and differences to PDE5. *Int J Impot Res*. 2004;16:S28–S33.
- Schudt C, Dent G, Rabe KF. *Phosphodiesterase Inhibitors*. New York: Academic Press; 1996.
- Manganiello V. Cyclic nucleotide phosphodiesterase 5 and sildenafil: promises realized. *Mol Pharmacol*. 2003;63:1209–1211.
- Lin CS, Xin ZC, Lin GT, Lue TF. Phosphodiesterases as therapeutic targets. *Urology*. 2003;61:685–691.
- Lincoln TM. Cyclic GMP and phosphodiesterase 5 inhibitor therapies: what's on the horizon? *Mol Pharmacol*. 2004;66:11–13.
- Lates AM, Zrenner E. Viagra (sildenafil citrate) and ophthalmology. *Prog Retin Eye Res*. 2002;21:485–506.
- Uckert S, Stief CG, Jonas U. Current and future trends in the oral pharmacotherapy of male erectile dysfunction. *Expert Opin Invest Drugs*. 2003;12:1521–1533.
- Gillespie PG, Beavo JA. Inhibition and stimulation of photoreceptor phosphodiesterases by dipyrindamole and M&B 22948. *Mol Pharmacol*. 1989;36:773–781.

15. Zhang J, Kuvelkar R, Wu P, Egan RW, Billah MM, Wang P. Differential inhibitor sensitivity between human recombinant and native photoreceptor cGMP-phosphodiesterases (PDE6s). *Biochem Pharmacol.* 2004;68:867-873.
16. Lipton SA, Rasmussen H, Dowling JE. Electrical and adaptive properties of rod photoreceptors in *Bufo marinus*. *J Gen Physiol.* 1977;70:771-791.
17. Capovilla M, Cervetto L, Torre V. Antagonism between steady light and phosphodiesterase inhibitors on the kinetics of the rod photoresponses. *Proc Natl Acad Sci USA.* 1982;79:6698-6702.
18. Rispoli G, Gillespie PG, Detwiler PB. Comparative effects of phosphodiesterase inhibitors on detached rod outer segment function. In: Borsellino A, Cervetto L, Torre V, eds. *Sensory Transduction*. New York: Plenum Press; 1990:157-167.
19. Lolley RN, Farber DB, Rayborn ME, Hollyfield JG. Cyclic GMP accumulation causes degeneration of photoreceptor cells: simulation of an inherited disease. *Science.* 1977;196:664-666.
20. Pentia DC, Hosier S, Colluppy RA, Valeriani BA, Cote RH. Purification of PDE6 isozymes from mammalian retina. *Methods Mol Biol.* In press.
21. Cote RH. Kinetics and regulation of cGMP binding to noncatalytic binding sites on photoreceptor phosphodiesterase. *Methods Enzymol.* 2000;315:646-672.
22. Cote RH, Biernbaum MS, Nicol GD, Bownds MD. Light-induced decreases in cGMP concentration precede changes in membrane permeability in frog rod photoreceptors. *J Biol Chem.* 1984;259:9635-9641.
23. Yoshikami S, Robinson WE, Hagins WA. Topology of the outer segment membranes of retinal rods and cones revealed by a fluorescent probe. *Science.* 1974;185:1176-1179.
24. Blazynski C, Cohen AI. Rapid declines in cyclic GMP of rod outer segments of intact frog photoreceptors after illumination. *J Biol Chem.* 1986;261:14142-14147.
25. Bownds D, Gordon-Walker A, Gaide Huguenin AC, Robinson W. Characterization and analysis of frog photoreceptor membranes. *J Gen Physiol.* 1971;58:225-237.
26. Pugh EN, Duda T, Sitaramayya A, Sharma RK. Photoreceptor guanylate cyclases: a review. *Biosci Rep.* 1997;17:429-473.
27. Dumke CL, Arshavsky VY, Calvert PD, Bownds MD, Pugh EN. Rod outer segment structure influences the apparent kinetic parameters of cyclic GMP phosphodiesterase. *J Gen Physiol.* 1994;103:1071-1098.
28. Cote RH, Brunnock MA. Intracellular cGMP concentration in rod photoreceptors is regulated by binding to high and moderate affinity cGMP binding sites. *J Biol Chem.* 1993;268:17190-17198.
29. Cheng Y-C, Prusoff WH. Relationship between the inhibition constant ( $K_i$ ) and the concentration of inhibitor which causes 50 per cent inhibition ( $IC_{50}$ ) of an enzymatic reaction. *Biochem Pharmacol.* 1973;22:3099-3108.
30. Mou H, Cote RH. The catalytic and GAF domains of the rod cGMP phosphodiesterase (PDE6) heterodimer are regulated by distinct regions of its inhibitory  $\gamma$  subunit. *J Biol Chem.* 2001;276:27527-27534.
31. D'Amours MR, Cote RH. Regulation of photoreceptor phosphodiesterase catalysis by its noncatalytic cGMP binding sites. *Biochem J.* 1999;340:863-869.
32. Ames A III, Barad M. Metabolic flux of cyclic GMP and phototransduction in rabbit retina. *J Physiol (Lond).* 1988;406:163-179.
33. Cervetto L, McNaughton PA. The effects of phosphodiesterase inhibitors and lanthanum ions on the light-sensitive current of toad retinal rods. *J Physiol (Lond).* 1986;370:91-100.
34. Polans AS, Kawamura S, Bownds MD. Influence of calcium on guanosine 3',5'-cyclic monophosphate levels in frog rod outer segments. *J Gen Physiol.* 1981;77:41-48.
35. Hodgkin AL, Nunn BJ. Control of light-sensitive current in salamander rods. *J Physiol (Lond).* 1988;403:439-471.
36. Cote RH. Structure, function, and regulation of photoreceptor phosphodiesterase (PDE6). In: Bradshaw RA, Dennis EA, eds. *Handbook of Cell Signaling*. San Diego: Academic Press; 2003:453-457.
37. D'Amours MR, Granovsky AE, Artemyev NO, Cote RH. The potency and mechanism of action of E4021, a PDE5-selective inhibitor, on the photoreceptor phosphodiesterase depends on its state of activation. *Mol Pharmacol.* 1999;55:508-514.
38. Huai Q, Liu Y, Francis SH, Corbin JD, Ke H. Crystal structures of phosphodiesterases 4 and 5 in complex with inhibitor 3-isobutyl-1-methylxanthine suggest a conformation determinant of inhibitor selectivity. *J Biol Chem.* 2004;279:13095-13101.
39. Cote RH, Bownds MD, Arshavsky VY. cGMP binding sites on photoreceptor phosphodiesterase: role in feedback regulation of visual transduction. *Proc Natl Acad Sci USA.* 1994;91:4845-4849.
40. Pugh EN Jr, Lamb TD. Amplification and kinetics of the activation steps in phototransduction. *Biochim Biophys Acta.* 1993;1141:111-149.
41. Corbin JD, Blount MA, Weeks JL, et al. [3H]sildenafil binding to phosphodiesterase-5 is specific, kinetically heterogeneous, and stimulated by cGMP. *Mol Pharmacol.* 2003;63:1364-1372.
42. Blount MA, Beasley A, Zoraghi R, et al. Binding of tritiated sildenafil, tadalafil, or vardenafil to the phosphodiesterase-5 catalytic site displays potency, specificity, heterogeneity, and cGMP stimulation. *Mol Pharmacol.* 2004;66:144-152.
43. Wensel TG, Stryer L. Reciprocal control of retinal rod cyclic GMP phosphodiesterase by its gamma subunit and transducin. *Prot Struct Funct Genet.* 1986;1:90-99.
44. Paglia MJ, Mou H, Cote RH. Regulation of photoreceptor phosphodiesterase (PDE6) by phosphorylation of its inhibitory  $\gamma$  subunit re-evaluated. *J Biol Chem.* 2002;277:5017-5023.
45. Sung BJ, Hwang KY, Jeon YO, et al. Structure of the catalytic domain of human phosphodiesterase 5 with bound drug molecules. *Nature.* 2003;425:98-102.
46. Artemyev NO, Natochin M, Busman M, Schey KL, Hamm HE. Mechanism of photoreceptor cGMP phosphodiesterase inhibition by its gamma-subunits. *Proc Natl Acad Sci USA.* 1996;93:5407-5412.
47. Granovsky AE, Artemyev NO. Identification of the  $\gamma$ -subunit interacting residues on photoreceptor cGMP phosphodiesterase, PDE6 $\alpha'$ . *J Biol Chem.* 2000;275:41258-41262.
48. Farber DB, Lolley RN. Cyclic guanosine monophosphate elevation in degenerating photoreceptor cells of the C3H mouse retina. *Science.* 1974;186:449-451.
49. Fox DA, Poblenz AT, He L. Calcium overload triggers rod photoreceptor apoptotic cell death in chemical-induced and inherited retinal degenerations. *Ann NY Acad Sci.* 1999;893:282-285.